Toxicology and Applied Pharmacology 283 (2015) 20–34

Contents lists available at ScienceDirect

Toxicology and Applied Pharmacology

journal homepage: www.elsevier.com/locate/ytaap

Evaluation of the fate and pathological response in the lung and pleura of brake dust alone and in combination with added chrysotile compared to crocidolite asbestos following short-term inhalation exposure

D.M. Bernstein [a,*], R.A. Rogers [b], R. Sepulveda [b], P. Kunzendorf [c], B. Bellmann [d,1], H. Ernst [d], O. Creutzenberg [d], J.I. Phillips [e]

[a] Consultant in Toxicology, Geneva, Switzerland
[b] Rogers Imaging, Needham, MA, USA
[c] GSA Gesellschaft für Schadstoffanalytik mbH, Ratingen, Germany
[d] Fraunhofer Institute for Toxicology and Experimental Medicine, Hannover, Germany
[e] National Institute for Occupational Health, National Health Laboratory Service, Johannesburg South Africa and Department of Biomedical Technology, Faculty of Health Sciences, University of Johannesburg, Johannesburg, South Africa

ARTICLE INFO

Article history:
Received 17 September 2014
Revised 26 November 2014
Accepted 23 December 2014
Available online 2 January 2015

Keywords:
Brake dust
Chrysotile
Crocdiolite asbestos
Fiber inhalation toxicology
Lung
Pleura

ABSTRACT

This study was designed to provide an understanding of the biokinetics and potential toxicology in the lung and pleura following inhalation of brake dust following short term exposure in rats. The deposition, translocation and pathological response of brake-dust derived from brake pads manufactured with chrysotile were evaluated in comparison to the amphibole, crocidolite asbestos. Rats were exposed by inhalation 6 h/day for 5 days to either brake-dust obtained by sanding of brake-drums manufactured with chrysotile, a mixture of chrysotile and the brake-dust or crocidolite asbestos. The chrysotile fibers were relatively biosoluble whereas the crocidolite asbestos fibers persisted through the life-time of the animal. This was reflected in the lung and the pleura where no significant pathological response was observed at any time point in the brake dust or chrysotile/brake dust exposure groups through 365 days post exposure. In contrast, crocidolite asbestos produced a rapid inflammatory response in the lung parenchyma and the pleura, inducing a significant increase in fibrotic response in both of these compartments. Crocidolite fibers were observed embedded in the diaphragm with activated mesothelial cells immediately after cessation of exposure. While no chrysotile fibers were found in the mediastinal lymph nodes, crocidolite fibers of up to 35 μm were observed. These results provide support that brake-dust derived from chrysotile containing brake drums would not initiate a pathological response in the lung or the pleural cavity following short term inhalation.

Introduction

The study is unique in that it has examined the pathological response and fiber distribution in the lung and in the pleural cavity of brake dust from chrysotile containing brake drums. In the interim results on the lung which were presented in Bernstein et al. (2014), the brake dust from chrysotile containing brake drums was shown to produce no pathological response in the lung through 91 days following short-term exposure in rats. The study also demonstrated the importance of amphibole asbestos exposure in comparison to chrysotile in the etiology of asbestos related lung disease. This study was continued through 365 days post exposure in order to assess the evolution of these findings and includes further results from the lung analyses and from the analysis of the pleural cavity from the study including assessment of the visceral and parietal pleural surfaces.

Chrysotile fibers were found to be effective since the 1900s in manufacturing brake materials with the ability to withstand heat and control speed. The surface of the brake drums often needed to be sanded to assure a proper fit. This study was designed to evaluate the hypothesis of whether brake dust from sanded chrysotile containing brake drums

Abbreviations: Crl: Wi(Han), Wistar rats, Specific Pathogen Free from Charles River Deutschland; SEM, scanning electron microscope; WHO, World Health Organization; MMMF, man made mineral fibers; VDI, Verein Deutscher Ingenieure (English, Association of German Engineers); GMD, Geometric mean diameter; GML, Geometric mean length; GSD, Geometric standard deviation; MMAD, Mass median aerodynamic diameter; %CT/FOV, percentage of the elastin and collagen per area of lung tissue; CM, Confocal microscopy; TGF-ß, Transforming growth factor (TGF)-β; bFGF, Basic fibroblast growth factor; PDGF, Platelet-derived growth factor; CTGF, connective tissue growth factor.

* Corresponding author. Fax: +41 22 735 1463.
E-mail addresses: davidb@itox.ch (D.M. Bernstein), rarogers5@yahoo.com (R.A. Rogers), Peter.Kunzendorf@GSA-Ratingen.de (P. Kunzendorf), Heinrich.ernst@item.fraunhofer.de (H. Ernst), jim.phillips@nioh.nhls.ac.za (J.I. Phillips).

[1] Deceased.

http://dx.doi.org/10.1016/j.taap.2014.12.012

will produce a pathological response following short term exposure in rats. Brake dust has not been previously evaluated in animal studies.

The techniques used in this study have been designed to sample the thin pleural surfaces with minimal alteration of the homeostatic balance and fiber location. Two independent methods were developed for examining the translocation of fibers to the pleural cavity and any associated inflammatory response following exposure to either brake dust with added chrysotile, brake dust alone or crocidolite asbestos. These methods included the in situ examination of the lungs and pleural space including the visceral and parietal pleural obtained from freeze substituted tissue in deep frozen rats and the examination of the diaphragm as a parietal pleural tissue.

In examining the visceral pleural environment, including the subpleural lung, the visceral pleural itself, and the pleural space, a non-invasive method for determining fiber location, size, inflammatory and fibrotic response was used on rats which were deep frozen immediately after killing. In addition, the visceral pleural wall thickness and the amount of collagen per field of view (fibrotic response) in the visceral pleura was quantified using confocal microscopy procedures.

The diaphragm was chosen as the parietal pleural tissue for examination because it can be quickly removed at necropsy with minimal alteration of the visceral lung surface and it has a high density of lymphatic stomata (Negrini et al., 1991; Negrini and Moriondo, 2013). A fixed area which included lymphatic drainage sites (stomata) on the diaphragmatic surface was selected for examination of possible inflammatory response using scanning electron microscopy (SEM) and for the presence of fibers.

Methods

The aerosol generation/exposure, in-life and pathology phases of this study were performed by the Fraunhofer Institute for Toxicology and Experimental Medicine (Hannover, Germany) in compliance with the Principles of Good Laboratory Practice (German Chemicals Act §19a, Appendix 1, July 02, 2008, Federal Law Gazette I, No. 28, p. 1146) and the German animal protection law (Tierschutzgesetz of May 18, 2006, German Federal Law Gazette I, page 1206, 1313). The fiber counting and sizing was performed by Gesellschaft für Schadstoffanalytik mbH (Ratingen, Germany). The confocal microscopy was performed by Rogers Imaging (Needham, Massachusetts, USA).

Brake dust

The brake dust was produced directly from chrysotile-containing friction products (automotive drum brake shoes) by the RJ LeeGroup Ltd. (Monroeville, PA, USA). The shoes were designed to fit the drum brakes of mid-1960's Chevrolet Impala model cars. The friction material was evaluated and found to contain approximately 30% (by area) chrysotile asbestos (analyzed in accordance with EPA 600/R-93/116). No amphibole asbestos minerals have been observed in any of the aerosol or lung samples from these brake shoes or in the added chrysotile used in this study.

The brake drums were ground using a commercial AMMCO arc grinder (Model 8000, S/N 24788) with a modified dust collection system. The arc grinder is a motorized sander that is swept across the surface of the brake shoe with the dust collected on an attached 8×10 inch quartz micro-fiber filter that was used in place of a collection bag. A Tisch high volume air sampler sampling pump (Tisch Environmental Inc., Ohio, USA) was used following the filter to provide uniform sampling suction over the course of the grinding operation. All brake dust preparation took place at the RJ LeeGroup facility in a room equipped with an Aramsco Comanche® HEPA ventilation unit (Model 55011) with a nominal flowrate of 1800 cfm (50 m^3/min). The brake dust was produced directly from asbestos-containing friction products (automotive drum brake shoes) by the RJ LeeGroup Ltd. (Monroeville, PA, USA) as described previously (Bernstein et al., 2014).

Chrysotile

The chrysotile fiber used in this study had the mineralogical grade of 5R04 according to the Canadian chrysotile asbestos classification (Cossette and Delvaux, 1979). The chrysotile grade 5R04 sample was chosen based upon an evaluation of which chrysotile grade was ordered or supplied for use in brake manufacturing in a random search of 67 formulations dating from 1964 to 1986. All of the grade 5R04 chrysotile in these brakes was supplied by Johns-Manville. The chrysotile sample used in this study was obtained directly from Mine Jeffery Canada (formerly the Johns-Manville Mine).

Crocidolite asbestos

The crocidolite asbestos sample used in this study was from the Voorspoed mine in South Africa was obtained from the National Institute of Occupational Health – NIOH, South Africa. This mine is located in Limpopo Province which at the time when mining took place was called Transvaal Province. The chemical compositions of chrysotile, a serpentine asbestos, and crocidolite, an amphibole asbestos, have been described previously (Shedd, 1985; Virta, 2002). A key difference with this crocidolite asbestos sample is that it was received as produced without subsequent grinding. The crocidolite asbestos used previously in animal studies has been largely either the Union for International Cancer Control (UICC) or US National Institute of Environmental Health Sciences (NIEHS) prepared crocidolite. Both of these samples were ground extensively more than 30 years ago using large scale industrial mills resulting in size distribution not typical of the commercial product (Bernstein et al., 2013).

Experimental design

The experimental design of the study has been illustrated in the flowchart in Fig. 1 of Bernstein et al., 2014. All end points were analyzed for each group with the exception that lung digestion was not performed in the control group on Days 1, 2 and 7 in order to limit animal use.

Animal exposure

Groups of laboratory rats (Groups 1, 2, 3 and 4) were exposed for 6 h per day for 5 days to:

Group 1: Filtered air (negative control group) (Total 65 animals).
Group 2: Brake dust powder mixed with chrysotile 5R04 (Total 100 animals).
Group 3: Brake dust powder (Total 100 animals).
Group 4: Crocidolite asbestos (Total 100 animals).

For groups 2 and 4, the exposure concentrations were set based upon the number of fibers longer than 20 μm/cm^3. In group 2, the chrysotile concentration was increased over that recommended by the EC Biopersistence Protocol (Bernstein and Riego-Sintes, 1999) of 100 fibers L > 20 μm/cm^3 due to the tendency of chrysotile to clump (this was minimized through the use of the cyclone, see below). Group 3 was included as a comparative exposure of the brake dust particulate material (with a relatively low aerosol concentration of chrysotile fibers) using a similar gravimetric exposure concentration as the brake dust component of group 2. A negative control group 1 was exposed in a similar fashion to filtered air.

Weanling (8–10 weeks old at exposure) male Wistar rats [Crl: WI(Han)], Specific Pathogen Free from Charles River Deutschland, Sulzfeld, Germany) were used. The rats were exposed by flow-past nose-only exposure for 6 h/day for a period of 5 consecutive days. In groups 2, 3, and 4; 7 animals per sub-group were allocated for lung burden evaluation at each time point. In the control group 1; 5 animals per sub-group were allocated for lung burden evaluation (no animals at days 1, 2 & 7). For the Confocal lung and histopathology, 3 animals per

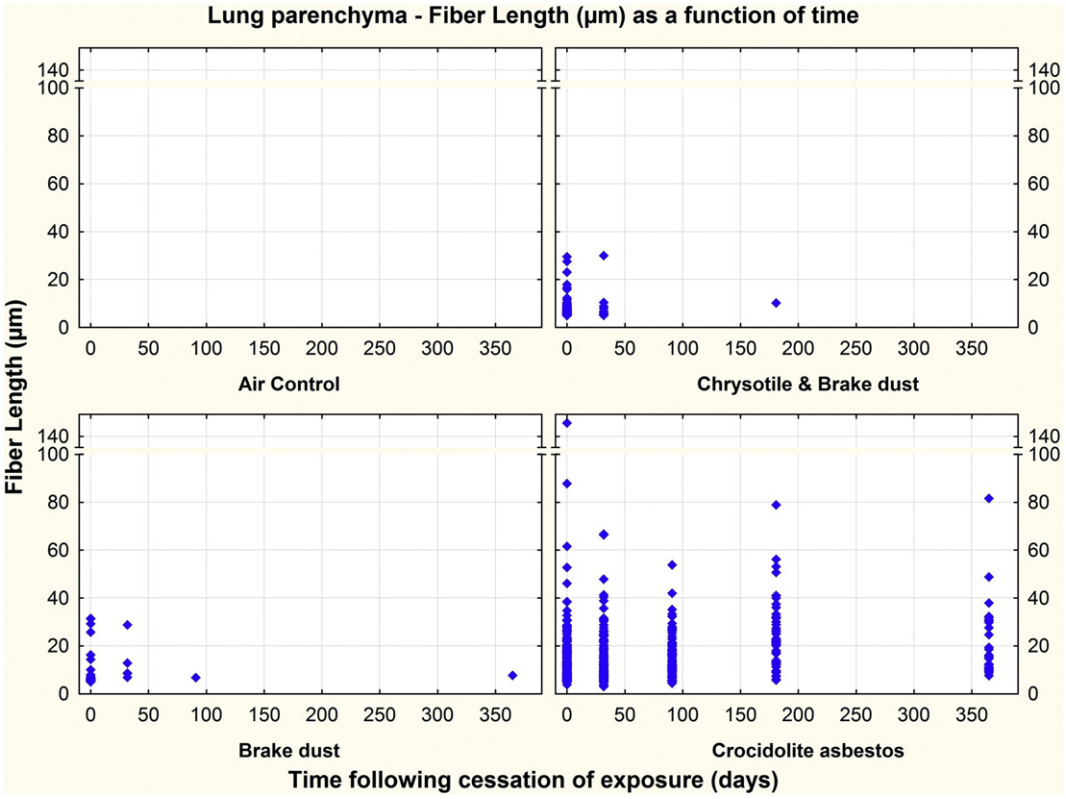

Fig. 1. Number and length of fibers observed in the lung parenchyma by confocal microscopy.

sub-group were allocated at each time point. For the low temperature Confocal microscopy, 3 animals per sub-group were allocated at each time point.

Exposure system

The fiber aerosol generation system (Model CR 3020, CR Equipments, Switzerland) was designed to loft the bulk fibers without breaking, grinding or contaminating the fibers (Bernstein et al., 1994). The animals were exposed using stainless steel flow-past nose/snout-only inhalation exposure systems with 16 animals per level. This system was derived from Cannon et al. (1983) and is different from conventional nose-only exposure systems in that fresh fiber aerosol is supplied to each animal individually and exhaled air is immediately exhausted. The exposure units were placed in separate ventilated chambers connected to the animal room to avoid cross contamination between the groups.

For group 2 (chrysotile fiber 5R04 mixed with brake dust powder), a fiber aerosol was generated from chrysotile fiber 5R04 and separately a dust aerosol from the brake dust using individual rotating brush aerosol generators (Bernstein et al., 2014). The fiber aerosol generator used was followed by a 500 mL pyrex glass cyclone to assist in the elimination of any remaining fiber bundles from the aerosol. The brake dust aerosol generator was followed by a micronising jet mill to reduce the particle size to be rat respirable. Following each generator, in-line ^{63}Ni charge neutralisers reduced the electrostatic charge from fibers and particulate material in the generated aerosols. Following the charge neutralizers, the fiber and powder aerosols were mixed through a Y-piece connection and then delivered directly into the nose-only flow-past exposure chamber. The group 3 brake dust aerosol was generated using only the 'powder aerosol generator'.

The group 4 crocidolite asbestos aerosol was generated using only the 'fiber aerosol generator'. A pre-study technical trial revealed stronger electrostatic properties of the crocidolite fiber aerosol which resulted in losses in the transfer tubing. To achieve a similar degree of neutralization with similar fiber transfer efficiency as with the chrysotile an electronic charge neutraliser at the brush head of the aerosol generator (WEKO Model AP230, Weitmann & Konrad GmbH, Germany) was used in addition to the ^{63}Ni charge neutraliser.

Exposure system monitoring

The aerosol concentration was monitored continuously using an aerosol photometer developed by Fraunhofer ITEM. Actual concentrations were measured in the breathing zone of the animals as described below. The temperature and the relative humidity of the exposure atmosphere were monitored continuously with data on temperature, relative humidity, and air flow rate collected by the Fraunhofer ITEM animal exposure facility computer system.

Gravimetric Determination of Aerosol Concentrations: Gravimetric determinations of aerosol concentration were performed at least once daily for each group with samples collected on a Millipore® glass fiber filter (Type 13400-25-J) for approximately 4–6 hours per day.

Fiber number and size distribution of Aerosol Concentrations: Aerosol samples for bivariate analysis of fiber size distribution and counting were collected onto NUCLEPORE® filters (PC membrane, 25 mm, pore size 0.8 µm – SN 110.609, Whatman Ltd.) for approximately 2 hours successively during each exposure period in parallel with the gravimetric sampling. For group 1 (air control) one sample per treatment day was collected over approximately 5 hours per day. These samples were analysed for bivariate fiber size distribution and counting (# fibers/cm^3 aerosol) using analytical Scanning Electron Microscopy (SEM) with Energy Dispersive x-ray analysis (EDAX).

Counting rules for the evaluation of air and lung samples by scanning electron microscopy (Fiber/Particle Analysis and Lung Digestion): Unless otherwise specified, the basis for the evaluation using the scanning electron microscope (SEM) was WHO-Reference Methods for measuring airborne man made mineral fibers (MMMF) WHO (1985) and the VDI Guideline 3492 (2004).

All objects seen at the magnification of 10,000× (acceleration voltage 25 kV) were sized with no lower or upper limit imposed on either length or diameter. The bivariate length and diameter was recorded individually for each object measured. Fibers were defined as any object that had an aspect ratio of at least 3:1. The diameter was determined at the greatest width of the object. All other objects were considered as non-fibrous particles. Fibers with both ends in the field of view had the "weight" of one fiber (=2 fiber ends), fibers with only one end within the field had the "weight" of a half fiber (=1 fiber end). Fibers without any fiber end in the field of view were not counted nor measured.

The stopping rules for counting each sample were defined as follows.

Fibrous objects: The minimum numbers of fibers examined were:

a) fibers with a length <5 μm = 100 fibers (200 fiber ends)
b) fibers with a length between 5 and 20 μm = 200 fibers (400 fiber ends)
c) fibers with a length >20 μm = 100 fibers (200 fiber ends)

Fields of view were examined for each length category until the defined minimum number of fibers for each length category was recorded or a maximum of 1 mm^2 of the filter surface was examined in case the fiber minimum number for the length category was not reached. For samples of the control group an area of 0.5 mm^2 of the filter was evaluated. These counting rules were based on the number of fibers per sample necessary in order to have statistical reproducibility of the means (EUR, 18748 EN, 1999). For non-fibrous objects, fields of view were examined until a total of 100 particles were recorded or the aforementioned stopping criteria for fibers were reached.

The details of the procedures for clinical examination and body weights; gross pathology and organ weights; tissue preparation for lung ashing; histopathology and for the confocal microscopy of the lung are presented in Bernstein et al., 2014.

Diaphragm tissue preparation

Diaphragms were excised from the chest wall, pinned flat to stiff filter paper with parietal surface facing up and immersion fixed in modified Karnovski's fixative. Specimens were then dispatched to Rogers Imaging Corporation (Needham Heights, MA, USA) for processing and analysis. Upon arrival, the fixed diaphragms were piece dissected by 10 mm biopsy punch, dehydrated and prepared for scanning electron microscopy.

Chest wall processing

For each chestwall a series of cross sectional slabs 4–5 mm thick were cut using a band saw. Slabs were placed on a dry ice cooled copper plate, then put into wire mesh processing baskets, labeled, and immersed by group in freeze-dry transition fluid (anhydrous methanol (75%), acetone (25%)) in 1 l cryo containers and stored at −80 °C. Cryo-fluids were replaced weekly for up to two months. Then specimens were stored in cryo-fluid at − 20 °C with weekly fluid replacement until solution cleared, usually after one month.

Staining and preparation of specimens for microscopic evaluation

Following freeze substitution, cross sections of chestwall were transferred to anhydrous methanol at −20 °C and brought to room temperature. Chestwall slabs and lung pieces were then stained with Lucifer yellow-CH (0.0001%) (Rogers et al., 1999), infiltrated in Spurr epoxy resin then heat cured. Undisturbed surfaces of chestwall slabs were exposed within the Epoxy embedment using a belt sander, or in the case of lung, 2 milimeter-thick sections were cut using a thin kerf rock saw blade. Exposed surfaces were polished using a diamond lapidary wheel until glass smooth.

Confocal microscopy

Confocal microscopy imaging was performed on chestwall slabs from each animal for each time point using Sarastro 2000 or 2010 (Molecular Dynamics, Inc.) laser scanning microscopes fitted with 25 mW argon-ion lasers and an upright Zeiss Axiophot or upright Nikon or inverted Nikon Diphot 2 microscopes, modified for reflected light imaging in dual channel reflected and fluorescent imaging mode. The cellular constituents and fibers (and particles) were imaged simultaneously with this arrangement with each "exposure" producing two digital images in perfect register with one another (Bernstein et al., 2010). Images were recorded through 60× objectives for Nikon-fitted confocal microscopes with voxel dimensions of 0.16 μm, 0.16 μm, and 0.60 μm (x, y, and z dimensions, respectively). Voxel dimensions were 0.16 μm, 0.16 μm, and 0.50 μm (x, y, and z dimensions, respectively) obtained from 63× objective for the Zeiss-fitted confocal microscope.

Mediastinal lymph nodes

One of the principle routes of clearance of the lymphatic fluid which is drained by the stomata on the parietal pleura is through the mediastinal lymph nodes. The mediastinal lymph nodes were collected at necropsy and pooled for each exposure group at each time point. They were then processed by lung digestion and then analyzed for fiber number and size distribution by SEM using similar procedures as was performed for the lung.

Statistical analyses

The confocal data was analyzed using analysis of variance (StatSoft, Inc. (2013) STATISTICA (data analysis software system), version 12 www.statsoft.com; MedCalc, ver 12.7, Ostend, Belgium). The fiber clearance half-times were calculated using StatSoft, Inc. (2013) and GraphPad Prism version 6.00 for Windows (GraphPad Software, La Jolla, CA, USA, www.graphpad.com).

Results

The validation of the lung digestion and counting procedures has been presented in Bernstein et al., 2014.

The exposure conditions are summarized in Table 1. The exposure conditions and the bivariate length and diameter distributions have been presented in Bernstein et al. (2014).

The fiber distribution in the chrysotile and brake dust aerosol included a larger number of shorter fibers with 84% less than 5 μm. For those fibers longer than 20 μm there was a mean of 189 fibers/cm^3 ranging from 20 to 160 μm in length. Of the long fibers, 99% were less than 1 μm in diameter (rat-respirable) with 95% less than 0.4 μm in diameter.

The crocidolite-exposure atmosphere had considerably fewer short fibers with 66% less than 5 μm. For those fibers longer than 20 μm there was a mean of 93 fibers/cm^3 ranging in length from 20 to 190 μm. 88% of the long fibers were less than 1 μm in diameter (rat respirable) with 21% of the fibers less than 0.4 μm in diameter.

In the brake dust exposure group there were fewer chrysotile fibers present without the added chrysotile with a mean of 3 fibers longer than 20 μm/cm^3. These longer fibers ranged in length from 20 to 140 μm with 90% less than 1 μm in diameter (rat respirable) with 63% of the fibers less than 0.4 μm in diameter.

Fiber clearance (from the lung digestion evaluation)

The fiber clearance was determined through 365 days post exposure using the whole lung digestion procedures described earlier (Bernstein et al., 2014). The clearance half-times based on the results through 91 days post exposure which were presented in that publication, have

Table 1
Aerosol concentration and size distribution of the exposure atmosphere in the air control group 1, chrysotile and brake dust group 2, brake dust group 3 and crocidolite asbestos group 4.

Exposure Group	Gravimetric Concentration mg/m^3 / SD	Total Number of Fibers counted on the filter*	Number of total fibers/cm^3	WHO Fibers/cm^3	Percent WHO fibers	Number of fibers ≥20 μm/cm^3	Percent of all fibers ≥20 μm/cm^3	Mean Number Particles/cm^3	Diameter Range (μm)	Length Range (μm)	GMD (μm) / GSD	GML (μm) / GSD	Mean Diameter (μm)/SD	Mean Length (μm)/SD	Length weighted arthm. diameter (μm)	Length weighted geom. diameter (μm)	Aspect ratio
(Group 1) Air Control	0	7	0.002	0.001	42.9	0	0	0.006	0.5–1.8	2.3–6.8	1.11 1.53	4.49 1.46	1.20 0.44	4.70 1.63	1.34	1.23	4.07
(Group 2) Chrysotile & Brake dust	3.48 0.36	2,454	6,953	1,007	14.5	189	2.7	3,140	0.03–2.4	0.6–160	0.17 1.68	2.47 2.32	0.20 0.12	4.01 6.83	0.19	0.16	29.8
(Group 3) Brake dust**	1.52 0.07	1,623	389.3	46.0	11.8	3.6	0.9	1240	0.05–2.9	0.6–140	0.21 1.79	2.25 2.00	0.25 0.20	3.21 4.25	0.32	0.24	16.99
(Group 4) Crocidolite	6.34 0.42	1,820	2,013	709	35.2	93	4.6	602	0.05–2.6	0.7–190	0.34 1.64	4.07 2.44	0.39 0.21	6.50 9.40	0.50	0.39	17.62

SD: Arithmetic standard deviation; GMD: Geometric mean diameter; GML: Geometric mean length; GSD: Geometric standard deviation; MMAD: Mass median aerodynamic diameter.
* The total number of fibers counted on the filter is based upon the rules specified in section "Fiber/Particle Analysis and Lung Digestion" above.
** For the brake dust group 3, the MMAD = 1.89 (Geometric standard deviation = 2.54) as determined by the impactor measurement.

been updated based upon the data through 365 days after cessation of exposure as shown below (Table 2).

The 5R04 grade of chrysotile used in the current study, according to the Quebec Standard Testing system (Cossette and Delvaux, 1979) this grade fiber had more than 60% of the fibers by weight larger than 0.13 cm (screen opening in the selection apparatus). Even though these bundles were largely separated prior to use in this study, 11% of the fibers > 1 μm in diameter were longer than 20 μm and ranged in length up to 51 μm. As presented in Bernstein et al. (2014) such fibers could become trapped in the lower airways and with the whole lung digestion procedure could not be differentiated in terms of location in the lung. The few longer fibers observed by confocal microscopy were observed in the airways. In addition, the large number of shorter fibers remaining in the lung accumulate preferentially in the lymphatic system which again cannot be differentiated through the lung digestion procedure. This resulted in group 2 in a two phase clearance and as such the weighted clearance half-time (as described in Bernstein and Riego-Sintes, 1999; Bernstein et al., 2001) was determined as shown in Table 2. As presented in Fig. 1, below, the confocal microscopy analysis confirmed that the long chrysotile fibers do not persist in the lung parenchyma.

Fiber clearance (from the confocal microscopy evaluation)

With the confocal microscopy examination of the lung parenchyma in which the amount of connective tissue (presented below) was determined, the number and length of any fiber in these regions was also determined. These results are shown in Fig. 1 with the summary statistics presented in Table S1 (supplemental data). In the brake dust with added chrysotile group as well as the brake dust alone group the fibers longer than 20 μm were rapidly cleared with only one fiber observed at 32 days post exposure and none thereafter. In the crocidolite asbestos exposed animals, numerous long fibers were observed which persisted through 365 days post exposure. The maximum crocidolite fiber length observed in the parenchyma was 146 μm.

Pathological findings in the lung

Histopathology

Histopathological findings reported earlier through 91 days after cessation of exposure clearly differentiated the response to brake dust with added chrysotile and brake dust alone as compared to crocidolite asbestos. The histopathological findings in the lung through 365 days are presented in Table S-2 with the key histopathological scores illustrated in Fig. 2. These results through 365 days post exposure continue to reinforce the differentiation between brake dust with added chrysotile and brake dust alone as compared to crocidolite asbestos.

There were no exposure-related histopathological findings in animals exposed to filtered air. In the chrysotile-brake dust group and brake dust alone group, slight accumulation of particle laden macrophages were observed from 7 through 91 days post exposure which decreased at 181 and 365 days post exposure. At 32 days post exposure, very slight (multi)focal particle laden micro-granulomas at the bronchiolo-alveolar junctions were observed in groups 2 and 3, however, there were no associated giant cells. There were no fiber related findings observed in groups 2 or 3 throughout the 365 day observation period.

In the crocidolite asbestos exposure group, accumulations of fiber laden macrophages were observed already at day 0, immediately following cessation of exposure. This incidence increased at day 7 and was associated with the formation of (multi)focal fiber laden micro-granulomas at the bronchiolo-alveolar junctions with multinucleate (syncytial) giant cells within these micro-granulomas. Interstitial fibrosis was observed by day 32. These findings persisted through 365 days post exposure. In addition, pleural fibrosis was also observed at 365 days post exposure in response to the crocidolite fibers.

Table 2
Estimated fiber clearance half times in days (through 365 days post exposure) (SE: standard error).

Group	Exposure	Fibers L > 20 μm	Fibers 5–20 μm	Fibers < 5 μm	Particles
		(days)			
2	Chrysotile & brake dust	42* (SE: 12)	52* (SE: 29)	109* (SE: 52)	399 (SE: 426)
3	Brake dust	29 (SE: 9)	46 (SE: 17)	54 (SE: 20)	110 (SE: 49)
4	Crocidolite asbestos**	>1000	>1000	>1000	>1000

SE: standard error.
* Weighted $T_{1/2}$ based on double exponential fit to the data (Bernstein and Riego-Sintes, 1999; Bernstein et al., 2001).
** The standard errors for the crocidolite estimates could not be calculated due to the lack of clearance.

Pulmonary fibrosis analysis – confocal microscopy

The connective tissue (elastin and collagen) present in the lung was measured by confocal microscopy to obtain the percentage of the elastin and collagen per area of lung tissue (%CT/FOV). These measurements were performed on the same lung parenchyma volumes which were examined for fiber length in Fig. 1. For each group and time point 300 cubic lung tissue volumes of 112,550 μm^3 each were imaged, the amount of connective tissue measured and the number and length of the fibers observed were recorded. Fields of view that contained a blood-vessel of diameter greater than 50 μm were not included due to the high amount of collagen in the blood-vessel walls.

The percent fibrosis is shown in Fig. 3 for each group at 0, 32, 91, 181 and 365 days after cessation of the 5 day exposure. The summary statistics are presented in Table S-3. In the air control group the percent connective tissue ranged from a mean of 3.8 ± 2.9 at day 0 to 7.1 ± 4.2 at day 365 with a range in individual values over this period of 0.1–24%. Compared to the air control group, there were no statistically significant (analysis of variance) trends in the chrysotile & brake dust group or in the brake dust group alone with or without fibers present. The chrysotile fibers present in the tissues had no impact on the development of connective tissue compared to the air control group and did not cause a fibrotic response through 365 days post exposure.

In the crocidolite asbestos exposure group, there is a consistent statistically significant increase in the mean amount of connective tissue present compared to day 0 (mean 4.5 ± 3.5) through 91 days post exposure (mean 14.7 ± 12.7) which then persisted through 365 days (mean 13.5 ± 8.9) as determined by analysis of variance. At 91 days, when compared to the air control group the mean connective tissue in the crocidolite asbestos exposure group increased by ~ 5 times.

The range of individual measurements shows that at day 0 the percent connective tissue in the crocidolite asbestos exposure group was similar to that found in the air control (0.2 - 23%), however, by 91 days post exposure, the connective tissue range in group 4 increased up to 87%.

Translocation of fibers to the pleural cavity and pathological response

One of the main objectives of this study was to examine the translocation of fibers to the pleural cavity using non-invasive techniques and to evaluate whether these fibers produce a pathological response.

Two methods were used to perform this analysis. The examination of the visceral pleural and the sub-visceral pleural regions of the lung was performed on the deep frozen tissues on subgroups of animals at 14, 91, 181 and 365 days post-exposure.

The examination of the diaphragm as a representative parietal pleural tissue was performed on the same animals that were examined for lung histopathology and CM. These animals were examined at time points starting at 0 days, immediately following cessation of exposure, through 365 days post-exposure. The 0 day results are presented here.

Visceral pleural examination and analysis

The visceral pleura barrier is a key boundary in the transport of fibers from the lung to the pleural cavity. Examination of the visceral pleural

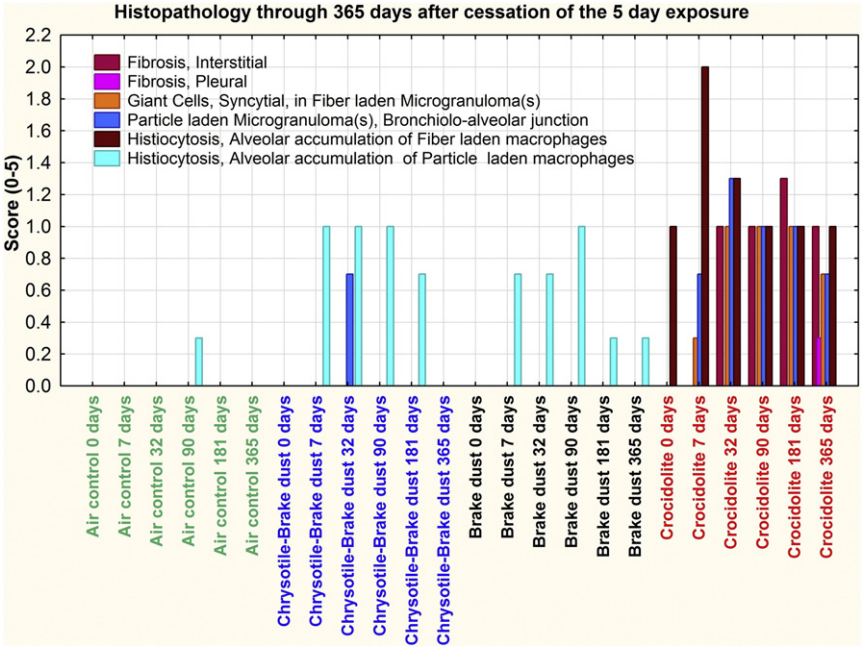

Fig. 2. Histopathological scores through 365 days after cessation of exposure.

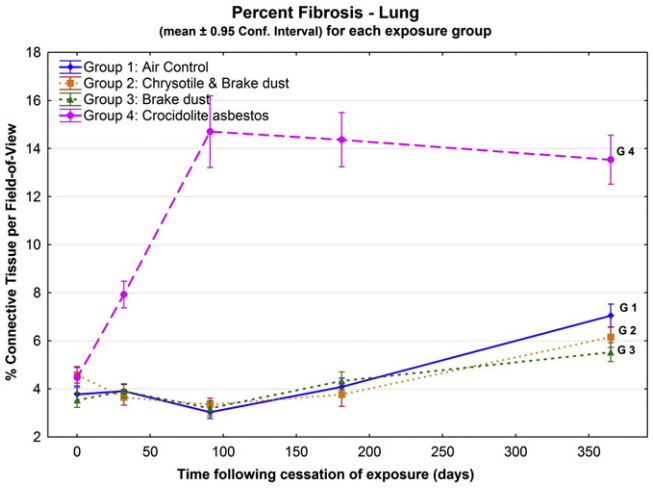

Fig. 3. Percent fibrosis (connective tissue per field of view) measured in the lung parenchyma by confocal microscopy.

region provides an initial and important indication of whether fibers reach this area and can produce pathological response.

The visceral pleural was systematically examined from cross-sections of rats that were frozen in liquid nitrogen immediately following sacrifice. This procedure was used in order to avoid possible artefacts that could stem from cross-contamination of fibers from the lung to the pleural cavity when tissues are manipulated at necropsy. The examination included a systematic survey using CM of the visceral pleural wall, the adjacent subpleural alveoli and the pleural space. The features of the tissues were evaluated and the location and length of any fibers present were determined.

In addition, the thickness of the pleural wall was measured at between 5 and 10 points in each section examined and the amount of collagen was quantified using the confocal microscopy procedures similar to which was reported above for the lung.

The visceral wall thickness is influenced by inflammation and fibrotic development. Disordered fibrin turnover plays a central role in the pathogenesis of pleural fibrosis (Bignon and Gee, 1985). A progression of increased vascular permeability, formation of a transitional fibrin gel, and remodelling and organization of the fibrinous neomatrix are common to the pathogenesis of lung inflammation and neoplasia, including tumors of the lung and pleural space (Idell et al., 2001).

As shown in Fig. 4 (summary statistics are presented in Table S-5), in the air control group, the mean visceral wall thickness ranges from 2.5 ± 0.6 μm on day 14–3.4 ± 0.7 μm on day 365 post exposure. For the chrysotile with brake dust and the brake dust alone groups there were no statistically significant differences (analysis of variance) between the mean visceral wall thicknesses as compared to the air control.

With the crocidolite asbestos exposure group a rapid increase in the mean visceral wall thickness was observed from 14 days through 272 days post exposure at which time it plateaued through 365 days post exposure. The mean visceral wall thickness in the crocidolite asbestos exposed rats increased from a mean on day 14 of 3.1 ± 0.7 μm to 5.8 ± 0.8 μm on day 272 which then persisted through day 365 (5.8 ± 2.0) and ranged from 2.9 μm to 19 μm.

The amount of connective tissue (elastin and collagen) present in the visceral pleura was also examined as to whether the increase in visceral pleura thickness was accompanied by an increase in collagen.

As shown in Fig. 5 (summary statistics are presented in Table S-6), the mean percent connective tissue per field of view was not statistically different in the chrysotile with added brake dust and the brake dust alone groups in comparison to the air control group (analysis of variance). In the crocidolite asbestos exposed group, the mean percent connective tissue per field of view increased from a mean of 6.5 ± 2.4% on day 14 to 16.1 ± 9.4% on day 365 which was statistically different from the air control and the brake dust groups (analysis of variance, $p < 0.01$). It is interesting to note that while the visceral pleural wall thickness levels off from 272 to 365 days post exposure, the percent connective tissue continued to increase indicative of a continuing inflammatory response to the crocidolite asbestos fibers.

With the confocal analysis of the chestwall, the length of any fibers observed within the fields of view analysed was also recorded. Fig. 6 shows length of each fiber observed in the visceral pleura space examined for thickness and percent connective tissue above (summary statistics are presented in Table S-7). No fibers were observed at any time point in the visceral pleura region of air control group and one short fiber of 3.3 μm was observed in the brake dust group at 365 days. In the chrysotile and brake dust group fibers up to 17.9 μm were observed at day 14, however, only 2 short fibers of 3 and 4.7 μm were observed at day 91 and at day 365 one fiber 4.3 μm was observed which is coherent with the disintegration of the longer chrysotile fibers and their subsequent clearance.

In the crocidolite asbestos exposed rats, fibers up to 26 μm were observed at 14 days post exposure with no systematic clearance of the fibers through 365 days post exposure. At 365 days post exposure, 15 fibers were observed in the visceral pleura region surveyed ranging in length up to 22.2 μm.

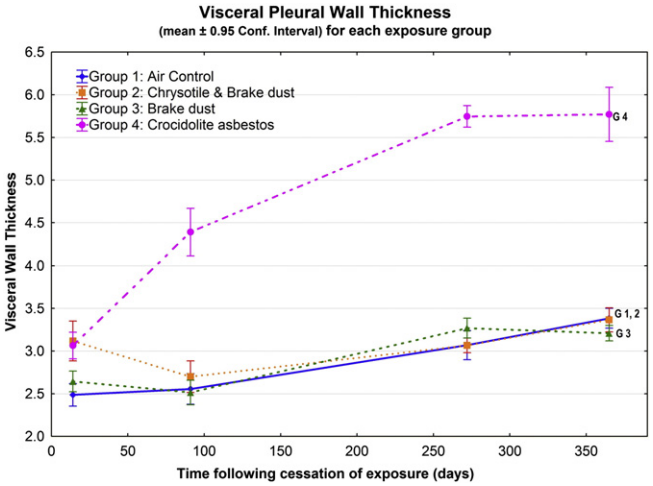

Fig. 4. Visceral pleural wall thickness measured by confocal microscopy.

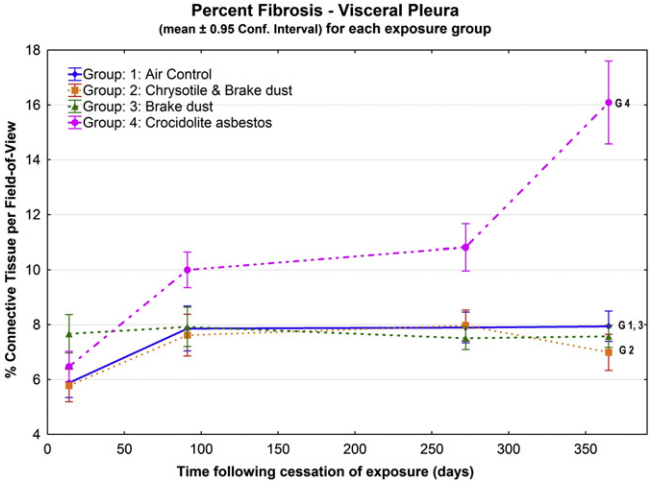

Fig. 5. Percent fibrosis (% conenctive tissue) in the visceral pleural wall measured by confocal microscopy.

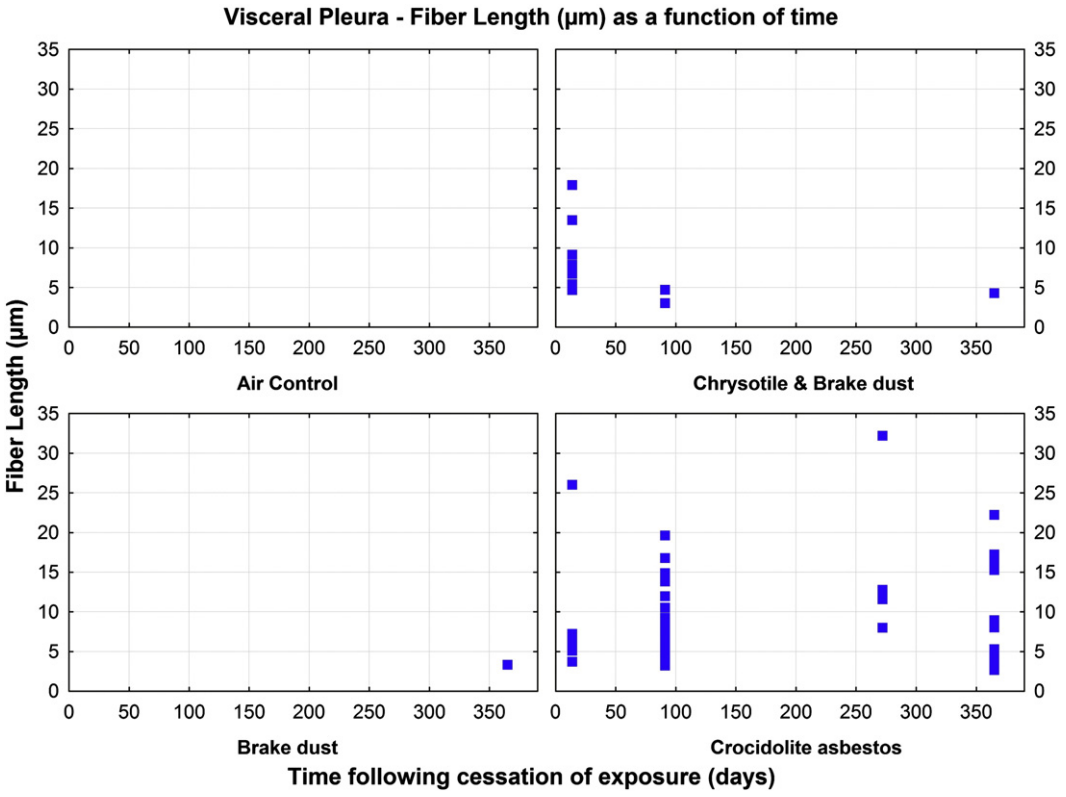

Fig. 6. Visceral pleural wall – number and length of fibers observed by confocal microscopy.

Mediastinal lymph nodes

One of the principle routes of clearance of the lymphatic fluid which is drained by the stomata on the parietal pleura is through the mediastinal lymph nodes (Negrini and Moriondo, 2013). The number and length and diameter distribution of the fibers present in the mediastinal lymph nodes is shown in Fig. 7 with the results summarized in Table S8. At 91 day after cessation of exposure, no chrysotile fibers were observed in the mediastinal lymph nodes of the brake dust or chrysotile/brake dust exposed groups. In the crocidolite exposed animals, at 91 days post exposure, a total of 58 crocidolite fibers were recovered from the mediastinal lymph nodes with lengths up to 35 µm (diameter 0.65 µm) and diameters up to 1.1 µm (length 8.7 µm).

Confocal microscopy images of the pleura

The snap frozen chest walls that were collected from animals in each of the exposure groups at 14, 91, 272 and 365 days following cessation of exposure were processed as described above and imaged using confocal microscopy. This process preserved the tissue, cellular and spatial orientation of any particles or fibers present in the visceral and parietal pleura as well as in the pleural space. There was some minor contraction of the lung during the snap freezing process which was observed in the wavy orientation of the visceral pleural surface.

The confocal microscopy images (Figs. 8–10) show the comparative response in the visceral and parietal pleura for each group. Sub pleural alveolar septa appear as grayscale in color. Visceral pleural surface and

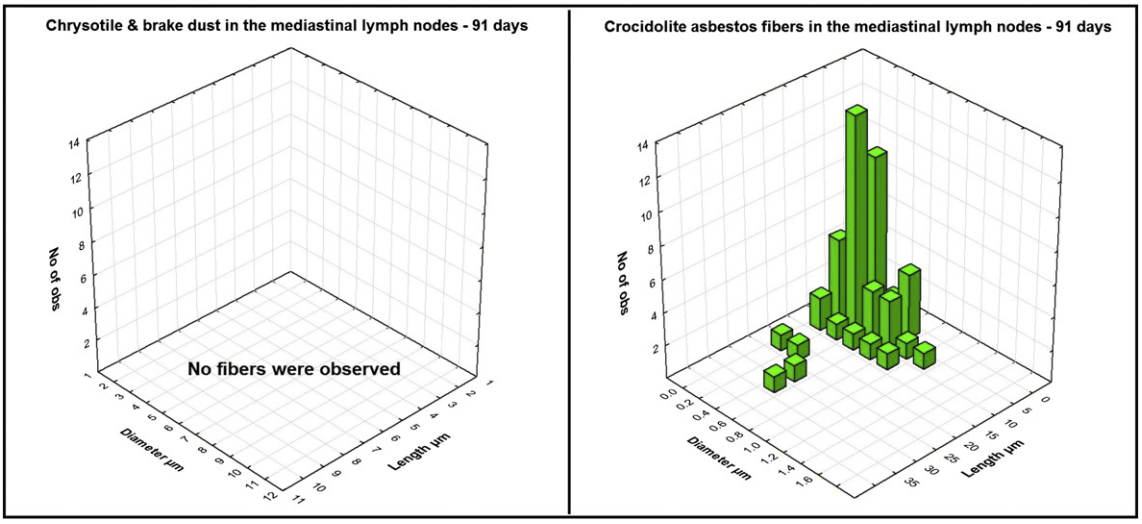

Fig. 7. Mediastinal lymph nodes — fiber length & diameter distribution at 91 days post exposure.

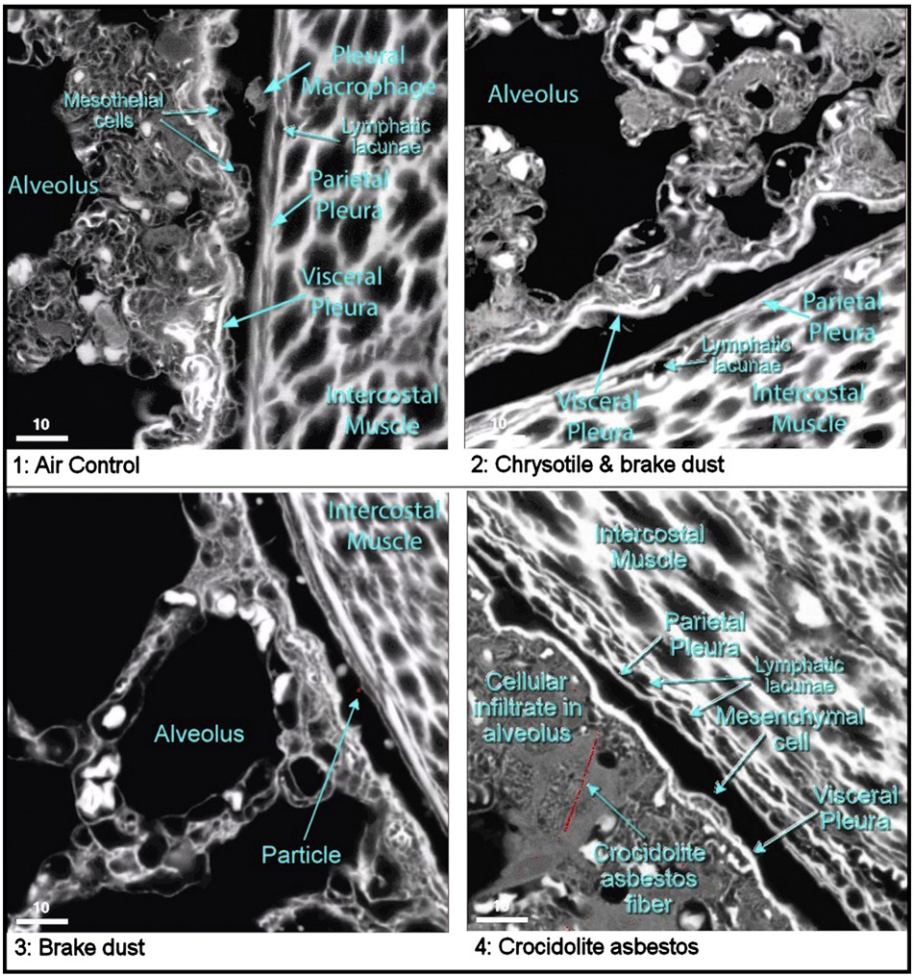

Fig. 8. Confocal images of the pleural cavity: 14 days after cessation of exposure. The images were obtained from snap frozen chestwall sections which preserved the tissue, cellular and spatial orientation of any particles or fibers present. The intercostal muscle which runs between the ribs and is mainly involved in the mechanical aspect of breathing is seen on the right, adjacent to the parietal pleura (when present). Opposite is the visceral pleura wall and the alveolar region of the lung. Details of each image are provided in the text.

(when present) parietal pleura surfaces high in collagen content appear as bright white linear profiles. Pleural space cells and particles and or fibers (red, if present) in context with lung tissue and pleura are also shown.

A typical image of the air control is shown in Fig. 8, panel 1 (14 days post exposure). The intercostal muscle which runs between the ribs and is mainly involved in the mechanical aspect of breathing is seen on the right, below the parietal pleura. Also indicated are submesothelial lymphatic lacunae into which the pleural fluid flows through the stomata. The pressure oscillations in the lacunae, related either to tissue motion or contractile properties of myogenic cells, represent the main mechanism for lymph propulsion toward larger lymphatic collecting ducts (Negrini et al., 1992). A pleural macrophage is observed within the pleural space. The normal collagen of the visceral pleura is observed as a solid white line on which can be seen mesothelial cells. Below the visceral pleura are the sub-pleural alveoli. Red blood cells can also be seen in the blood vessels surrounding the alveoli.

At 14 days following exposure to brake dust with added chrysotile (Fig. 8, panel 2), the visceral and parietal pleura, sub-pleural alveoli and pleural space have nearly the same appearance as the air control group. Similarly, the brake dust exposed group has a similar appearance with the exception of a single particle in the pleural space (Fig. 8, panel 3). No fibers were observed.

At 14 days following the end of exposure to crocidolite asbestos, a very different image is observed (Fig. 8, panel 4). A long crocidolite asbestos fibers (~25 μm) can be seen within a sub-pleural alveolus adjacent to the visceral pleura. Partial profiles of a number of other fibers can also be seen. A dense cellular infiltrate fills the alveolus and the surrounding alveoli. On the visceral pleura, a mesenchymal cell can be observed. Below the parietal pleura, the lymphatic lacunae which drain the pleural fluid through the stomata appear enlarged suggestive of increased pleural fluid flow.

At 91 days after cessation of exposure, the visceral and parietal pleura architecture of the brake dust with added chrysotile and the brake dust group alone appears similar to that of the air control group (Fig. 9, plates 1–3). In the brake dust group, a particle is seen adjacent to a pleural macrophage. No fibers were observed.

In the crocidolite asbestos exposure group at 91 days post exposure (Fig. 9, plate 4), a crocidolite fiber is seen within the pleural space. In addition, numerous pleural macrophages and neutrophils are also present surrounded by greyish wisps, which is likely coalesced pleural protein that was a result of the freezing process. Activated mesothelium is seen on the visceral pleura, which now has a dense collagen matrix (bright white area). The parietal pleura is not seen in this image.

At 272 and 365 days after cessation of exposure images of only the crocidolite asbestos exposure group are shown (Fig. 10) as the brake dust with added chrysotile and the brake dust group alone continue to appear similar to that of the air control group. In Fig. 10, plate 1, a crocidolite fiber is observed in the sub-pleural alveolus around which a granuloma has formed with a collagen capsule around the fiber. In Fig. 10, plate 2, an extended collagen matrix is seen along the visceral pleura. The parietal pleura is activated with enlarged mesothelial

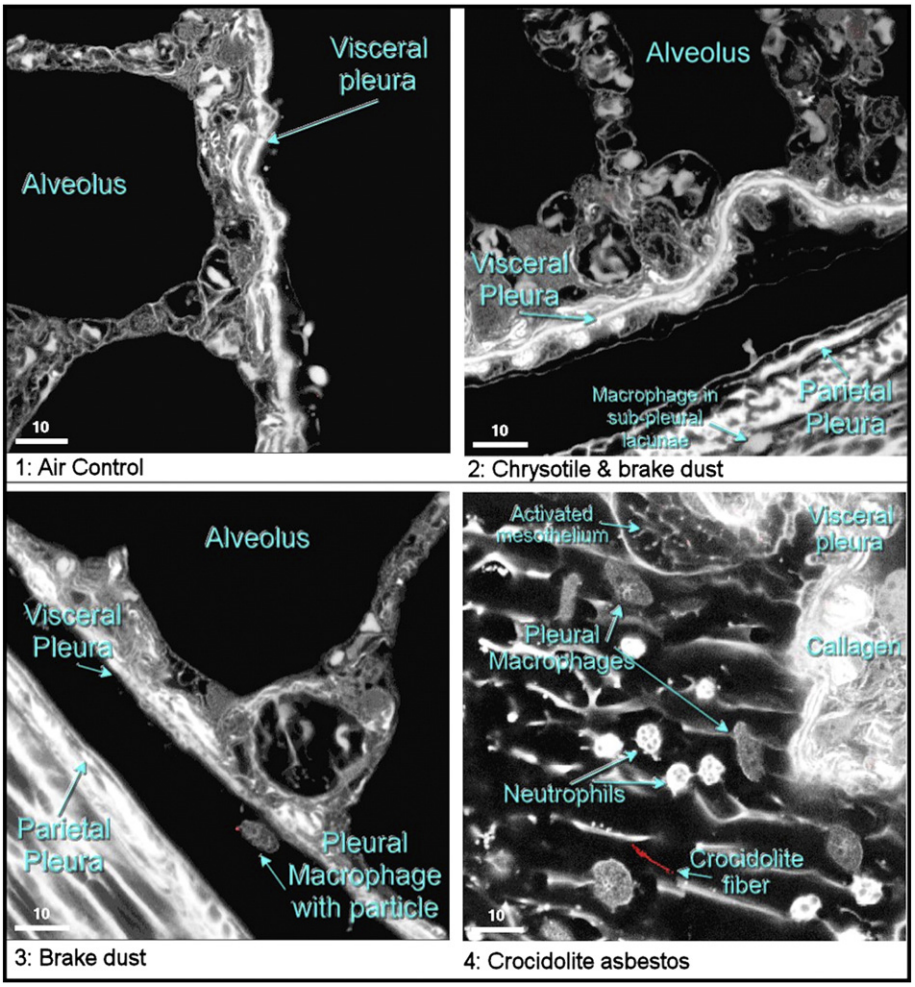

Fig. 9. Confocal images of the pleural cavity: 91 days after cessation of exposure: The images were obtained from snap frozen chestwall sections which preserved the tissue, cellular and spatial orientation of any particles or fibers present. The intercostal muscle which runs between the ribs and is mainly involved in the mechanical aspect of breathing is seen on the right, adjacent to the parietal pleura (when present). Opposite is the visceral pleura wall and the alveolar region of the lung. Details of each image are provided in the text.

cells with philapodia extensions. The sub-pleural lymphatic lacunae are again enlarged suggestive of a continuing increase in pleural fluid flow.

At 365 days post exposure (Fig. 10, plate 3) a crocidolite fiber is observed in the dense collagen matrix of the visceral pleura. In addition, there is a strong localized protein response adjacent to the visceral pleura. The parietal pleura is not shown in this image. In Fig. 10, plate 4, both the visceral and parietal pleura have extensive collagen networks with fibrin adhesions bridging the visceral and parietal pleura.

Parietal pleura (diaphragm) examination

The lymphatic stomata on the diaphragm represent a major site for pleural and peritoneal liquid drainage (Negrini et al., 1991). The diaphragm was chosen as a representative parietal pleura sample as it also could be readily removed from the animal quickly after sacrifice thus reducing the possibility of contamination through post-mortem body fluids.

Scanning electron microscopy was included to image the surface of the diaphragm and confocal microscopy to image the sub-pleural structure. Thus far, the SEM images at 0 days after cessation of exposure are available as shown in Fig. 11. The brake dust with added chrysotile and the brake dust alone were found to be similar in appearance to the air control group. Shown in each of these images are lymphatic stomata which are the parietal pleura lymphatic drainage portals.

In the crocidolite asbestos exposed group, immediately following cessation of the 5 day exposure, two crocidolite fibers are observed sticking out of the diaphragmatic surface (plate 4). These fibers are likely embedded in the stomata one of which is partially seen below the lower fiber. Activated mesothelial cells are also observed in the vicinity of these fibers. Two additional SEM images of the diaphragm from the crocidolite asbestos group at day 0 are shown in Fig. 12. Plate 1 shows a cluster of neutrophils on the mesothelial parietal surface. Plate 2 shows a 5.3 μm crocidolite fiber being transported by the mesothelial microvilli towards a stomata. What is notable is that there is no mesothelial activation or inflammatory cells present in response to this short fiber.

Discussion

While our understanding of fiber pathogenesis continues to evolve, this study confirms the importance of fiber characteristics on the potential for producing a pathological response following inhalation. The biosolubility of the chrysolite fibers appears to affect their clearance and toxicity, especially the initial inflammatory response and tissue injury, and the resulting fibrogenic response. Chrysotile is a thin rolled sheet of magnesium on the outside and silica on the inside which is acid soluble (Kobell, 1834; Whittaker, 1957, 1963; Tanji et al., 1984; Titulaer et al., 1993). In contrast, amphibole asbestos fibers such as

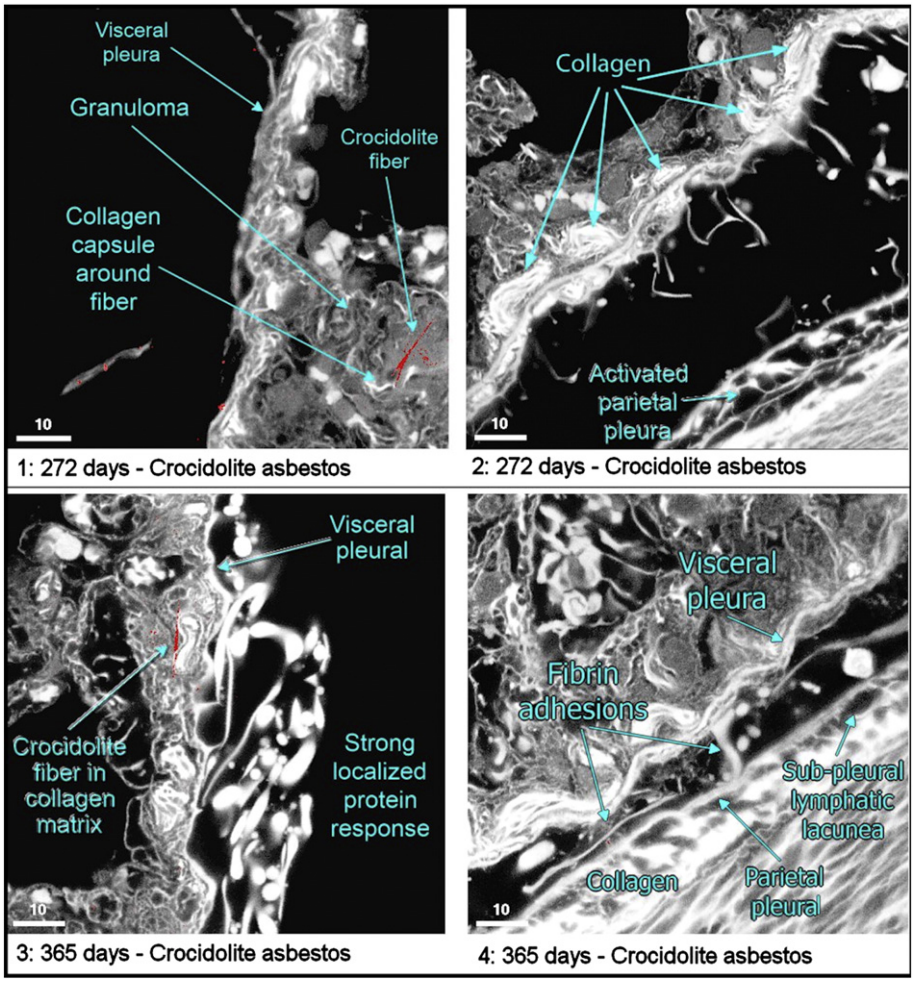

Fig. 10. Confocal images of the pleural cavity: Crocidolite asbestos 272 and 365 days after cessation of exposure: The images were obtained from snap frozen chestwall sections which preserved the tissue, cellular and spatial orientation of any particles or fibers present. The intercostal muscle which runs between the ribs and is mainly involved in the mechanical aspect of breathing is seen on the right, adjacent to the parietal pleura (when present). Opposite is the visceral pleura wall and the alveolar region of the lung. Details of each image are provided in the text.

crocidolite, are encased in silica and are insoluble at any pH that can occur in physiological conditions (Skinner et al., 1988; Whittaker, 1960).

This is the first study to assess the effects of chrysotile containing brake-dust. This study is also unique in that it included as a positive control a crocidolite sample that was not previously ground in preparation and thus contained a fiber size distribution more typical of what would have been encountered in commercial use.

The aerosol exposures to the chrysotile fibers used in this study were well above those that have been reported historically for mechanics working with brakes. Paustenbach et al. (2003) reviewed the historical exposures of mechanics to asbestos in brake dust and reported that the estimated and measured 8-hour time weighted averages (TWAs) for mechanics servicing automobiles and light trucks ranged from <0.002 to 0.68 f/cm^3, with a mean of 0.04 f/cm^3. The personal sampling data on which these TWAs were based showed that the concentrations ranged from <0.004 to 2.33 f/cm^3. For mechanics servicing heavy truck and bus brakes, the 8-hour TWAs ranged from 0.002 to 1.75 f/cm^3, with a mean of 0.2 f/cm^3. The corresponding personal sample concentrations ranged from <0.004 to 7.09 f/cm^3.

Blake et al. (2003) evaluated the dust emissions from four nearly identical automobiles from 1960s that were fitted with new replacement asbestos-containing brake shoes and then driven over a predetermined public road course for about 2253 km. Each car was brought separately into a repair facility; the brakes removed and replaced with new asbestos-containing shoes that were filed, sanded and ground as required. The authors reported that the airborne chrysotile fiber exposures for each test remained below currently applicable limit of 0.1 fiber/ cm^3 (eight-hour time-weighted average). The authors also measured the total dust for brake changing tests expressed as 8-h TWA that ranged from 0.193 to 0.708 mg/m^3 with a mean of 0.333 mg/m^3. The cleaning test resulted in less than 0.102 mg/m^3 total dust exposure. The respirable dust fraction expressed as 8-h TWA indicated concentrations below the 0.095 mg/m^3 detection limit for all but filing and the second arc-grinding tests, where 0.243 and 0.103 mg/m^3 were found, respectively. The mean respirable dust exposure concentration was <0.121 mg/m^3 or about one third of that for the total dust.

In this study the chrysotile aerosol exposure concentration was 1,007 f(WHO)/cm^3 in the combined chrysotile and brake dust group 2 and 46 f(WHO)/cm^3 in the brake dust group 3. Compared to the historical mean TWA for servicing automobiles and light trucks of 0.04 f/cm^3, the chrysotile fiber exposure concentration in group 2 of this study was 25,000 times the mean historical TWA exposure. The mean respirable gravimetric dust exposure concentration in this study was 3.48 mg/m^3 for group 2 and 1.52 mg/m^3 for group 3. Compared to the historical mean gravimetric TWA concentration for changing brakes of <0.121 mg/m^3, the gravimetric exposure concentration in group 2 of this study was more than 29 times the mean historical gravimetric exposure.

The estimated clearance times of the fibers >20 μm from the lung through 365 days were 42 days for the chrysotile and brake dust group and 29 days for the brake dust alone group. In comparison to

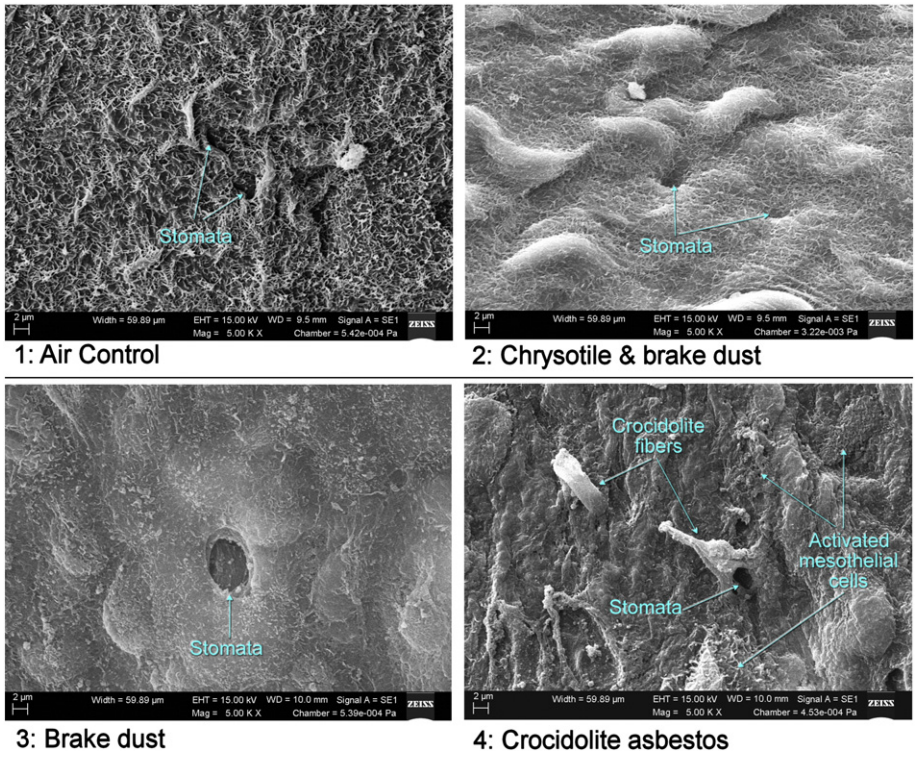

Fig. 11. Scanning electron micrographs of the diaphragm at 0 days following cessation of exposure. Exposure groups 1–4 are shown in each of the corresponding plates. Plates 1, 2, and 3 show a normal diaphragm structure with a stomata. Plate 4 shows crocidolite fibers penetrating the stomata of the diaphragm with adjacent activated mesothelial cells.

the crocidolite asbestos exposure group which had an estimated clearance half-time >1000 days, the longer chrysotile fibers cleared rapidly. Chrysotile can vary in characteristic depending upon the mine and processing of the ore. In earlier studies of chrysotile alone or of chrysotile mixed with a joint compound (Bernstein et al., 2003, 2004, 2005a, 2005b, 2008, 2011) the clearance half-time of the longer fibers ranged from 0.7 to 11.4 days. The lack of a fiber related response in the histopathological findings in either the lung or the pleural cavity strongly suggests that the few (group 2: 6.5–10 fibers counted on the filter; group 3: 1–5 fibers counted on the filter) remaining fibers longer than 20 μm in the current study were in the airways and not in the parenchyma. The clearance half-time of fibers longer than 20 μm that were less than 1 μm in diameter was 1.6 days for the chrysotile and brake dust group which is within the range of the earlier studies.

With the crocidolite asbestos exposure group 4, following the early clearance of the shorter fibers most likely from the tracheobronchial region, the intense inflammatory response induced by the longer fibers effectively locked-up further clearance. For all fibers lengths there was no subsequent clearance and the clearance half-time was estimated as greater than 1000 days. In previous biopersistence studies with amphibole asbestos, the clearance half-time was reported to range from 418 to >1000 days (Musselman et al., 1994; Hesterberg et al., 1996, 1998; Bernstein et al., 2005b, 2011).

The biopersistence study on amosite asbestos reported by Musselman et al. (1994) and Hesterberg et al. (1996, 1998) did not evaluate histopathological response or fiber translocation to the pleura. The Bernstein et al. (2005b) study which included tremolite asbestos did examine the histopathological response in the lung. The authors reported that following 5 days of exposure tremolite asbestos produced a pronounced inflammatory response with the rapid development of granulomas followed by the development of fibrosis characterized by collagen deposition within these granulomas and by 90 days even mild interstitial fibrosis. In the Bernstein et al. (2011) study amosite asbestos was evaluated as a positive control. The study was designed to evaluate the pathological response

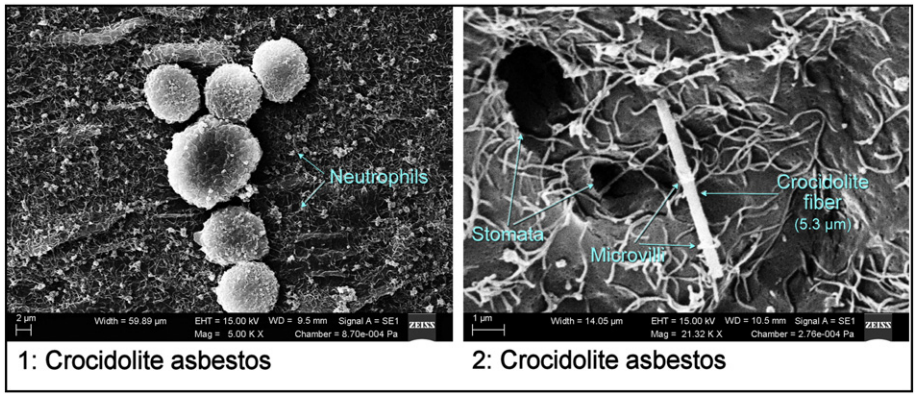

Fig. 12. Scanning electron micrographs of the diaphragm at 0 days following cessation of exposure. Crocidolite asbestos exposure group. Plate 1 shows neutrophils of the surface of the diaphragm. Plate 2 shows a 5.3 μm crocidolite fiber supported by the mesothelial microvilli adjacent to a stomata.

and fiber distribution within the lung and pleural cavity. The authors reported that amosite fibers were found to remain partly or fully imbedded in the interstitial space through 1 year and quickly produced granulomas (0 days) and interstitial fibrosis (28 days). Amosite fibers were observed penetrating the visceral pleural wall and were found on the parietal pleural within 7 days post-exposure with a concomitant inflammatory response seen by 14 days. In this study, the visceral wall thickness was measured for the first time using confocal microscopy. There was no difference in visceral wall thickness between the air control group and a group exposed to chrysotile mixed with sanded joint compound. In contrast the amosite asbestos exposed group had more than twice the visceral wall thickness.

In the current study, the design has been further enhanced with the inclusion of the measurement of not only the visceral wall thickness but also the quantification of collagen in the lung and in the visceral pleural wall. In the brake dust and the brake dust with added chrysotile groups, there was no inflammatory response to the chrysotile and no increase in connective tissue in the lung in comparison to the air control group. The only finding reported was a mild macrophage response to the particles present.

In contrast, in the crocidolite asbestos exposure group, the accumulation of fiber laden macrophages observed immediately following cessation of exposure quickly progressed to interstitial fibrosis by seven days and which persisted through 365 days post exposure at which time pleural fibrosis was also observed. There was a linear increase in fibrotic response in the lung parenchyma through 91 days post exposure after which the level of fibrotic response persisted through 365 days post exposure. The mean visceral pleural wall thickness increased by 180% through 272 days post exposure with a doubling in the amount of collagen present at 365 days.

The confocal images of the pleural cavity and the visceral and parietal pleural walls as well as the SEM images of the parietal pleural (diaphragm), provide a comparative basis for the observations reported in this study in comparison to those described in the scientific literature.

One of the goals of this study was to provide insight into the translocation of fibers from the lung to the pleural cavity through the use of non-invasive techniques. While between the lung and the visceral pleura wall there is a network of lymphatic capillaries and collecting vessels, the larger sub-visceral lymphatic vessels contain one-way valves, directing flow of lymph away from the pleura towards the hilar regions of the lung (Bernaudin and Fleury, 1985) and suggesting that this would not be a primary route of entry of fibers into the pleural cavity. Crocidolite fibers are observed in the sub pleural alveoli as well in the visceral pleural region. Due to the rapid onset of inflammatory response from these fibers it is likely that they have deposited following inhalation directly in these areas. What is remarkable in this study is the rapidity in which the crocidolite fibers can penetrate into the pleura and lodge in the stomata of the parietal pleural surface initiating an inflammatory response as observed immediately after the termination of the five day exposure. This was not observed for the brake dust and chrysotile fibers.

It appears that once fibers reach the pleural cavity, the pleural fluid which is produced by the parietal pleura, originating from the systemic circulation, is resorbed mainly through lymphatic drainage via the stomata exclusively on the parietal pleural side (Rahman and Wang, 2008). This flow would result in crocidolite fibers present in the pleural cavity entering the stomata and if they are either too large or are initiating an inflammatory response getting blocked at this point.

From the stomata the lymphatic drainage is facilitated by the lymphatic lacunae which are located in the sub-mesothelial region of the parietal pleura and with the movement of breathing serve to pump the lymph (Negrini et al., 1992; Negrini and Moriondo, 2011). Negrini and Moriondo (2011) have described how the initial lymphatics run through sub-mesothelial connective tissue composed of loose collagen fibers organized in bundles adjacent to the skeletal muscular fibers and that these contain two types of unidirectional valves which regulates fluid entrance into the lumen (Galie and Spilker, 2009) and prevents fluid back-flow (Negrini et al., 1992; Negrini and Moriondo, 2011, 2013).

In the rat, Parungo et al. (2005) have shown that the mediastinal lymph nodes are the sentinel lymph nodes of the pleural space. This study is also unique in assessing fiber number and dimensions in the mediastinal lymph nodes. At 91 days post exposure to crocidolite, fibers up to 35 μm were found in the mediastinal lymph nodes while no chrysotile fibers were observed.

The mesothelial cells which line the pleura are covered with microvilli and have been shown to phagocytize foreign substances such as bacteria, mineral particles such as asbestos fibers and quartz or latex beads (Jaurand and Fleury-Feith, 2008). The microvilli are associated with pinocytotic vessels, implying an important role in transcellular transport (Madison et al., 1979) and have a role in enmeshing glycoproteins rich in hyaluronic acid to lubricate the pleural surface and lessen friction between the lung and thorax (Andrews and Porter, 1973). Images in the current study show that the microvilli can encircle the shorter crocidolite fibers and appear to function to transport fibers towards the stomata as part of the clearance mechanism similar to the cilia in the tracheal bronchial tree. This transport of shorter fibers appears to occur without inducing an inflammatory response.

The mesothelial cell plays a critical role in the initiation of inflammatory responses in the pleural space because it is the first cell to recognize a perturbation in the pleural space. When activated, these cells recruit inflammatory cells (such as neutrophils) and release growth factors for fibroblasts which can lead to subsequent pleural fibrosis (Jantz and Antony, 2006). As observed in this study crocidolite fibers deposit in the stomata, activate the mesothelial cells on the pleural surface and result in the development of pleural fibrosis. This fibrotic response increased over time through the end of the post exposure observation period at 365 days where there was twice the connective tissue present compared to the air control (16.1 vs 7.9%). There was no statistically significant difference between the air control and brake dust and brake dust/chrysotile exposed groups with only a slight increase noted over this same time most likely due to aging.

Conclusions

This study has demonstrated that there is an important difference in the persistence, translocation and pathological response in the lung and in the pleura between brake dust derived from brakes manufactured with chrysotile compared to the amphibole, crocidolite asbestos. The pathological response was determined using two independent methods. Classical histopathological examination was performed on thin lung sections including visceral pleura with scoring of the collagen level at the bronchoalveolar junctions as well as the Wagner score. In addition, the collagen deposition in the connective tissue of the lung and visceral pleura was evaluated using confocal microscopy in order to assess the fibrotic response.

No significant pathological response was observed at any time point in the brake dust or chrysotile/brake dust exposure groups through 365 days post exposure. Slight macrophage accumulation was noted in response to the high particle exposure levels in the test atmospheres and the decomposition of the longer chrysotile fibers into shorter fibers or particles. This was reflected as well in the Wagner score which ranged from 1 to 2 (with one being the level in the air control group) (Bernstein et al., 2014). The long chrysotile fibers cleared quickly with clearance halftimes estimated as 29 and 42 days respectively in the brake dust and the chrysotile/brake dust exposure group.

This is the first study to quantify the rapid response to fibers and inflammatory development in the pleural cavity following inhalation of crocidolite asbestos and not chrysotile.

Using the quantitative evaluation of fibrotic response in the lung and in the visceral pleura with confocal microscopy, there was no statistically significant difference between the air control group and either the brake dust alone or the brake dust with chrysotile exposure group at

any time point through 365 days after cessation of exposure. In addition, the pleural wall thickness was also not statistically different between these groups.

The crocidolite asbestos produced inflammatory response in the lung parenchyma from day 0 which progressed to Wagner grade 4 interstitial fibrosis within 32 days following cessation of exposure. In addition, the confocal microscopy evaluation of the fibrotic response in the connective tissue showed a marked increase in fibrotic response through 91 days after cessation of exposure (4.8× air control) which persisted through 365 days post exposure. The long crocidolite fibers had a pulmonary clearance half-time of greater than 1000 days.

This study also quantified the evolution of the visceral wall thickness and fibrosis in response to the inhalation of crocidolite asbestos. The pleural wall thickness showed a steady increase through 365 days post exposure. This was accompanied by a corresponding increase in fibrotic response of the visceral pleural wall to 200% that of the air control at 365 days post exposure. The confocal microscopy showed the concomitant inflammatory response in the pleural cavity with the development of the fibrotic response in the pleural walls. In addition, the crocidolite fibers were shown to persist in the vicinity of the visceral pleural wall, and were observed in the pleural space and immediately after the cessation of the five-day exposure on the diaphragm blocking lymphatic stomata. This was accompanied by activation of mesothelial cells, the presence of neutrophils and macrophages and inter-wall adhesions similar to that described in the literature for humans exposed to amphibole asbestos.

There are many brake linings still in use worldwide that contain chrysotile. This study in rats provides in-vivo toxicological support that brake dust derived from chrysotile containing brake drums would not initiate a pathological response in the lung or the pleural cavity following short term inhalation.

Conflict of interest statement

This study was funded by Honeywell International Inc. The affiliations of the authors are as shown on the cover page and include research laboratories, government institute, corporate affiliations, as well as independent toxicology consultant. This publication is the professional work product of the authors and may not represent the views of the corporate sponsor. The role of the corporate sponsor was limited to provide study funding, identifying the brake dust test article, and supplying the brakes used in the study. There have been periodic communications between Honeywell and the authors concerning the status of this study. One of the authors, David Bernstein, has appeared as an expert witness in litigation concerned with alleged health effects of exposure to chrysotile. Honeywell is a defendant in asbestos-product litigation and its predecessor manufactured the automotive brakes used in this study. The contribution of Prof JI Phillips is based on research supported by the National Research Foundation.

Acknowledgments

This study was funded by Honeywell International Inc.

Appendix A. Supplementary data

Supplementary data to this article can be found online at http://dx.doi.org/10.1016/j.taap.2014.12.012.

References

Andrews, P.M., Porter, K.R., 1973. The ultrastructural morphology and possible functional significance of mesothelial microvilli. Anat. Rec. 177 (3), 409–426 (Nov).

Bernaudin, J.F., Fleury, J.Y., 1985a. Anatomy of the blood and lymphatic circulation of the pleural serosa. In: Chretien, J., Bignon, J., Hirsch, A. (Eds.), The pleural in health and disease. Marcel Dekker, New York, pp. 101–124.

Bernstein, D.M., Riego-Sintes, J.M.R., 1999. In: Bernstein, D.M., Riego-Sintes, J.M.R. (Eds.), European Commission Joint Research Centre, Institute for Health and Consumer Protection, Unit: Toxicology and Chemical Substances, European Chemicals Bureau. Methods for the determination of the hazardous properties for human health of man made mineral fibers (MMMF) vol. EUR 18748 EN (April 93. Available from: http://ecb.ei.jrc.it/DOCUMENTS/Testing-Methods/mmmfweb.pdf).

Bernstein, D.M., Mast, R., Anderson, R., et al., 1994. An experimental approach to the evaluation of the biopersistence of respirable synthetic fibers and minerals. Environ. Health Perspect. 102 (Supplement 5), 15–18.

Bernstein, D.M., Riego Sintes, J.M., Ersboell, B.K., Kunert, J., 2001. Biopersistence of synthetic mineral fibers as a predictor of chronic inhalation toxicity in rats. Inhal. Toxicol. 13 (10), 823–849 (Oct).

Bernstein, D.M., Rogers, R., Smith, P., 2003. The biopersistence of Canadian chrysotile asbestos following inhalation. Inhal. Toxicol. 15, 101–128.

Bernstein, D.M., Rogers, R., Smith, P., 2004. The biopersistence of Brazilian chrysotile asbestos following inhalation. Inhal. Toxicol. 16, 745–761.

Bernstein, D.M., Rogers, R., Smith, P., 2005a. The biopersistence of Canadian chrysotile asbestos following inhalation: final results through 1 year after cessation of exposure. Inhal. Toxicol. 17, 1–14.

Bernstein, D.M., Chevalier, J., Smith, P., 2005b. Comparison of *Calidria chrysotile* asbestos to pure tremolite: final results of the inhalation biopersistence and histopathology following short term exposure. Inhal. Toxicol. 17, 427–449.

Bernstein, D.M., Donaldson, K., Decker, et al., 2008. A biopersistence study following exposure to chrysotile asbestos alone or in combination with fine particles. Inhal. Toxicol. 20, 1009–1028.

Bernstein, D.M., Rogers, R.A., Sepulveda, R., Donaldson, K., Schuler, D., Gaering, S., Kunzendorf, P., Chevalier, J., Holm, S.E., 2010. The pathological response and fate in the lung and pleura of chrysotile in combination with fine particles compared to amosite asbestos following short-term inhalation exposure: interim results. Inhal. Toxicol. 22 (11), 937–962 (Sep).

Bernstein, D.M., Rogers, R.A., Sepulveda, R., et al., 2011. Quantification of the pathological response and fate in the lung and pleura of chrysotile in combination with fine particles compared to amosite-asbestos following short-term inhalation exposure. Inhal. Toxicol. 23, 372–391.

Bernstein, D., Dunnigan, J., Hesterberg, T., Brown, R., Velasco, J.A., Barrera, R., Hoskins, J., Gibbs, A., 2013. Health risk of chrysotile revisited. Crit. Rev. Toxicol. 43 (2), 154–183 (Feb).

Bernstein, D.M., Rogers, R., Sepulveda, R., Kunzendorf, P., Bellmann, B., Ernst, H., Phillips, J.I., 2014. Evaluation of the deposition, translocation and pathological response of brake dust with and without added chrysotile in comparison to crocidolite asbestos following short-term inhalation: interim results. Toxicol. Appl. Pharmacol. 276 (1), 28–46 (Apr 1).

Bignon, J., Gee, J.B.L., 1985. Pleural fibrogenesis. In: Chretien, J., Bignon, J., Hirsch, A. (Eds.), the Pleura in Health and Disease. Marcel Dekker, New York, pp. 417–443.

Blake, C.L., Van Orden, D.R., Banasik, M., Harbison, R.D., 2003. Airborne asbestos concentration from brake changing does not exceed permissible exposure limit. Regul. Toxicol. Pharmacol. 38 (1), 58–70 (Aug).

Cannon, W.C., Blanton, E.F., McDonald, K.E., 1983. The flow-past chamber: an improved nose-only exposure system for rodents. Am. Ind. Hyg. Assoc. J. 44 (12), 923–928.

Cossette, M., Delvaux, P., 1979. Technical evaluation of chrysotile asbestos ore bodies. In: Ledoux, R.C. (Ed.), Short course in mineralogical techniques of asbestos determination. Mineralogical Association of Canada, Toronto, Canada, pp. 79–109 (May).

EUR 18748 EN, 1999. In: Bernstein, D.M., Riego-Sintes, J.M.R. (Eds.), Methods for the determination of the hazardous properties for human health of man made mineral fibers (MMMF) vol. EUR 18748 EN. European Commission Joint Research Centre, Institute for Health and Consumer Protection, Unit: Toxicology and Chemical Substances, European Chemicals Bureau (April. 93, http://ecb.ei.jrc.it/DOCUMENTS/Testing-Methods/mmmfweb.pdf).

Galie, P., Spilker, R.L., 2009. A two-dimensional computational model of lymph transport across primary lymphatic valves. J. Biomech. Eng. 131, 1–9.

Hesterberg, T.W., Miiller, W.C., Musselman, R.P., et al., 1996. Biopersistence of man-made vitreous fibers and crocidolite asbestos in the rat lung following inhalation. Fundam. Appl. Toxicol. 29 (2), 269–279.

Hesterberg, T.W., Chase, G., Axten, C., et al., 1998. Biopersistence of synthetic vitreous fibers and amosite asbestos in the rat lung following inhalation. Toxicol. Appl. Pharmacol. 151 (2), 262–275.

Idell, S., Mazar, A.P., Bitterman, P., Mohla, S., Harabin, A.L., 2001. Fibrin turnover in lung inflammation and neoplasia. Am. J. Respir. Crit. Care Med. 163 (2), 578–584 (Feb).

Jantz, M.A., Antony, V.B., 2006. Pleural fibrosis. Clin. Chest Med. 27 (2), 181–191 (Jun).

Jaurand, M.C., Fleury-Feith, J., 2008. Mesothelial cells. In: Light, R.W., Lee, Y.C.G. (Eds.), Textbook of pleural diseases, 2nd ed. Arnold Hodder, London, UK, pp. 27–37 (ISBN13: 978-0-340-94017-4).

Kobell, F., 1834. Ueber den schillernden Asbest von Reichenstein in Schlesien. J. Prakt. Chem. 2, 297–298.

Madison, L.D., Bergstrom-Porter, B., Torres, A.R., Shelton, E., 1979. Regulation of surface topography of mouse peritoneal cells. Formation of microvilli and vesiculated pits on omental mesothelial cells by serum and other proteins. J. Cell Biol. 82 (3), 783–797 (Sep).

Musselman, R.P., Miiller, W.C., Eastes, W., et al., 1994. Biopersistences of man-made vitreous fibers and crocidolite fibers in rat lungs following short-term exposures. Environ. Health Perspect. 102 (Suppl. 5), 139–143.

Negrini, D., Moriondo, A., 2011. Lymphatic anatomy and biomechanics. J. Physiol. 589 (Pt 12), 2927–2934 (Jun 15).

Negrini, D., Moriondo, A., 2013. Pleural function and lymphatics. Acta Physiol. (Oxf.) 207 (2), 244–259 (Feb).

Negrini, D., Mukenge, S., Del Fabbro, M., Gonano, C., Miserocchi, G., 1991. Distribution of diaphragmatic lymphatic stomata. J. Appl. Physiol. 70 (4), 1544–1549 (Apr).
Negrini, D., Del Fabbro, M., Gonano, C., Mukenge, S., Miserocchi, G., 1992. Distribution of diaphragmatic lymphatic lacunae. J. Appl. Physiol. (1985) 72 (3), 1166–1172 (Mar).
Parungo, C.P., Colson, Y.L., Kim, S.W., Kim, S., Cohn, L.H., Bawendi, M.G., Frangioni, J.V., 2005. Sentinel lymph node mapping of the pleural space. Chest 127 (5), 1799–1804 (May).
Paustenbach, D.J., Richter, R.O., Finley, B.L., Sheehan, P.J., 2003. An evaluation of the historical exposures of mechanics to asbestos in brake dust. Appl. Occup. Environ. Hyg. 18 (10), 786–804 (Oct).
Rahman, N.M., Wang, N.S., 2008. Anatomy of the pleura. In: Light, R.W., Lee, Y.C.G. (Eds.), Textbook of pleural diseases, 2nd ed. Arnold Hodder, London, UK, pp. 13–25 (ISBN13: 978-0-340-94017-4).
Rogers, R.A., Antonini, J.M., Brismar, H., Lai, J., Hesterberg, T.W., Oldmixon, E.H., Thevenaz, P., Brain, J.D., 1999. In situ microscopic analysis of asbestos and synthetic vitreous fibers retained in hamster lungs following inhalation. Environ. Health Perspect. 107 (5), 367–375 (May).
Shedd, K.B., 1985. Fiber dimensions of crocidolites from Western Australia, Bolivia, and the Cape and Transvaal provinces of South Africa. U.S. Bureau of Mines Report of Investigations 8998. United States Department of the Interior.
Skinner, H.C.W., Ross, M., Frondel, C., 1988. Asbestos and other fibrous materials – mineralogy, crystal chemistry, and health effects. Oxford University Press, New York (NY).
Tanji, T., Yada, K., Akatsuka, Y., 1984. Alternation of clino- and orthochrysotile in a single fiber as revealed by high-resolution electron microscopy. Clay Clay Miner. 32 (5), 429–432.
Titulaer, M.K., van Miltenburg, J.C., Jansen, J.B.H., et al., 1993. Characterization of tubular chrysotile by thermoporometry, nitrogen sorption, drifts, and TEM. Clay Clay Miner. 41, 496–513.
VDI Guideline 3492, 2004. Indoor air measurement, ambient air measurement, measurement of inorganic fibrous particles, scanning electron microscopy method. Verein Deutscher Ingenieure e.V., Düsseldorf.
Virta, R.L., 2002. Asbestos: geology, mineralogy, mining, and uses. Prepared in cooperation with Kirk-Othmer encyclopedia of chemical technology. USGS Open file 02-149 Online edition. Wiley-Interscience, a division of John Wiley & Sons, Inc., New York (NY).
Whittaker, E.J.W., 1957. The structure of chrysotile. V. Diffuse reflexions and fiber texture. Acta Crystallogr. 10, 149–156.
Whittaker, E.J.W., 1960. The crystal chemistry of the amphiboles. Acta Crystallogr. 13, 291–298.
Whittaker, E.J.W., 1963. Research report: Chrysotile fibers – filled or hollow tubes? Mathematical interpretation may resolve conflicting evidence. Chem Eng News 41, pp. 34–35 (September 30, 1963).
WHO, 1985. Reference methods for measuring airborne man-made mineral Fiber (MMMF). WHO/EURO MMMF Reference Scheme. Prepared by the WHO/EURO Technical Committee for Monitoring and Evaluating Airborne MMMF. World Health Organisation, Copenhagen.